3. J.-Y. Sze and K.-L. Wong, Slotted rectangular microstrip antenna for bandwidth enhancement, IEEE Trans Antennas Propag 48 (2000), 1149–1152.
4. W.X. Zhang, C.S. Pyo, S.I. Jeon, S.P. Lee, and N.H. Myung, A new type of wideband slot-fed U-slotted patch antenna, Microwave Opt Technol Lett (1999), 378–381.
5. K. Mandal and P.P. Sarkar, High gain wide-band u-shaped patch antennas with modified ground planes, IEEE Trans Antennas Propag 61 (2013), 2279–2282.
6. K. Mondal and P.P. Sarkar, Design of compact broadband high gain microstrip patch antennas with modified ground plane, Microwave Opt Technol Lett 56 (2014), 1255–1259.
7. K. Mondal and P.P. Sarkar, A high gain broadband circular patch antenna with spiral shaped slot loaded modified ground plane, Microwave Opt Technol Lett 56 (2014), 2024–2046.

FIBER OPTIC DISPLACEMENT SENSOR BASED ON A DOUBLE-REFLECTING OTDR TECHNIQUE

Maria Thereza M. Rocco Giraldi,[1,2] Cindy S. Fernandes,[2,3] Marta S. Ferreira,[2,4] Marco J. de Sousa,[3] Pedro Jorge,[2] João C. W. A. Costa,[3] José L. Santos,[2,4] and Orlando Frazão[2,4]
[1] Department of Electrical Engineering, Military Institute of Engineering, Praça Gen Tiburcio, 80, Rio de Janeiro 22,290-270, Brazil; Corresponding author: mtmrocco@ime.eb.br
[2] INESC Porto, Porto 4169-007, Portugal
[3] Department of Electrical Engineering, Federal University of Pará, Campus do Guamá, Belém, 66,075–970, Brazil
[4] Department of Physics, Faculty of Sciences, University of Porto, Porto 4169-007, Portugal

Received 27 October 2015

ABSTRACT: *In this work, it is proposed a technique to implement an intensity sensor based on the generation of a double-reflecting (ghost) signal in optical time domain reflectometry (OTDR). The intensity sensor is supported by a singlemode-multimode-singlemode (SMS) fiber structure combined with a fiber loop mirror (FLM). The results of the displacement sensitivity show linear behavior for both the first-reflecting and double-reflecting signals with linear slopes of approximately −4.5 dB/mm and −6 dB/mm, respectively. The displacement resolution achieved is ∼0.28 mm. It is also found that the system is able to read periodic displacement variations in the millisecond time scale applied to the sensing head.* © 2015 Wiley Periodicals, Inc. Microwave Opt Technol Lett 57:1312–1315, 2015; View this article online at wileyonlinelibrary.com. DOI 10.1002/mop.29086

Key words: *optical fiber sensor; fiber loop mirror; interrogation system; optical time domain reflectometer*

1. INTRODUCTION

Optical time domain reflectometer (OTDR) is the most used optoelectronic equipment to measure distributed losses in single mode optical fibers [1]. The concept is based on Rayleigh scattered light, which permits to determine the attenuation of optical fiber links. OTDR is also useful to localize events, breaks and to evaluate fusion splices and optical connectors [1–3]. Due to these advantages and as OTDR is a simple, easy and ready to be used tool, it has also been the starting point when considering distributed sensing [2].

Due to the operation principle of the OTDR, if there is a high reflection from any point of the tested optical fiber, a generation of a double-reflecting "ghost" peak may appear in the OTDR trace [4]. When the OTDR sends a test pulse down the fiber, a high reflection from the far end comes back (if the pulse power is sufficiently high or the fiber is not long enough to attenuate the optical reflection below a certain level) and it shows up on the trace as an overloaded reflection [4]. Then, it may be reflected from the OTDR fiber link connector interface back down the fiber for a second round, effectively becoming a second "test pulse" which is again reflected back from the far end, returning to the OTDR to be recorded as a second trace [4]. If the reflections are high enough, this process can go on three or more times, each one producing a ghost event on the OTDR trace [4]. The ghost event can be mitigated and even canceled if the input signal is reduced or low reflection optical interfaces are implemented. Although the ghost signal is generally harmful for the OTDR operation, it can be a useful tool in optical sensors applications. In this case, the signal propagates in two-ways down the fiber duplicating the sensitivity.

Multimode interference effects occurring in singlemode-multimode-singlemode (SMS) fiber structures have been investigated as a mechanism for sensing [5], in some cases combined with OTDR supported interrogation techniques. It is the case of a recent experimental investigation addressing temperature measurement using the SMS structure as the temperature sensor and interrogated by an OTDR [6]. Here, we proceed with this research path, but now exploring the characteristics associated with the processing of the OTDR ghost signal, enhanced by considering a fiber loop mirror (FLM) at the far end of the fiber, with the sensing device for intensity measurement based on a SMS structure.

2. EXPERIMENTAL SETUP AND DISCUSSION

Figure 1 illustrates the experimental setup of the proposed technique. A commercial OTDR from YOKOGAWA, model AQ 1200 OTDR—Multi Field Tester is used to interrogate the intensity sensor. The OTDR optical source is a multimode laser, operating at 1550 nm, with 2 μs pulse width and 2.5 dB input signal attenuation. Remote sensing is obtained connecting 11.6 km of Corning SMF-28 fiber to the OTDR port.

The intensity sensor is based on a SMS structure, formed by a short section of a multimode fiber, with 105/125 μm core/cladding diameters, a step refractive index profile and 3 mm length, sandwiched and spliced to two SMF-28 fibers, 9/125 μm core/cladding diameters. The 3 mm length was chosen as it enables high sensitivity for the intensity sensor. Although, it is not an easy task to cleave and splice the 3 mm long MMF to the SMF fibers, the sensor is perfectly reproducible. The SMS structure is illustrated in Figure 2(a) and the setup where the SMS structure is fixed is shown in Figure 2(b).

Different from a multimode interference structure, the SMS sensor operation is not dependent on the wavelength and merely introduces a loss in the optical signal, as can be observed in the optical spectra shown in Figure 3. In this case, a broadband source illuminated the SMS structure and a displacement from 0 to 400 μm was applied on it. The optical spectrum is attenuated

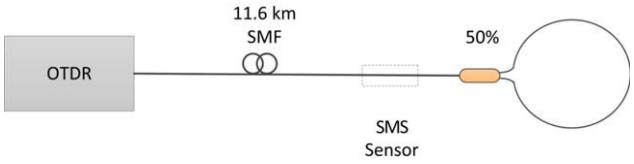

Figure 1 Experimental setup of the proposed sensing technique. [Color figure can be viewed in the online issue, which is available at wileyonlinelibrary.com]

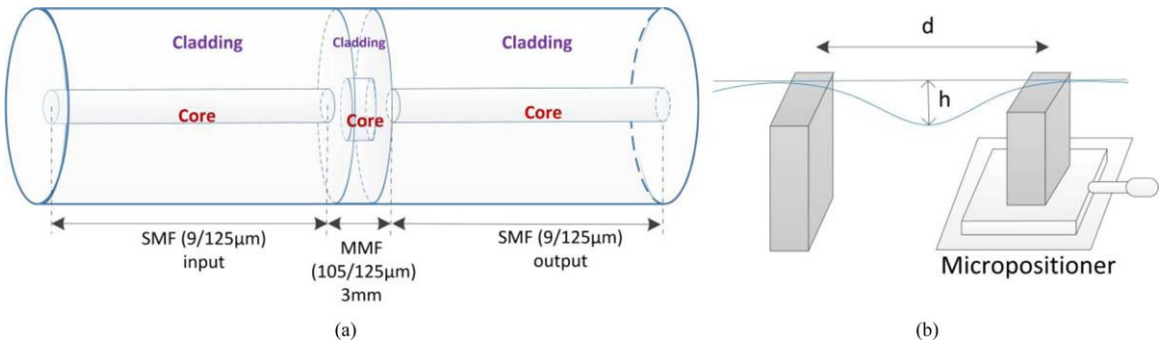

Figure 2 (a) SMS structure and (b) setup which permits to introduce the displacement in the sensor. [Color figure can be viewed in the online issue, which is available at wileyonlinelibrary.com]

but it does not change with wavelength as the curvature is applied.

A FLM is connected to the output of the intensity SMS sensor to increase the reflected ghost signal [7]. The FLM is straightforward developed using a 3 dB optical coupler. In this case, the 1.5 m output ports of the coupler are spliced together forming a loop. All light input to the loop is reflected back to the coupler input port due to constructive interference, which occurs in the coupler after the counter waves propagate inside the loop [1, 8, 9]. As the output ports present short fiber lengths and no pulse duration is altered, the FLM behaves linearly [10]. The FLM permits to generate a strong reflection peak, as it provides almost 100% signal power reflection (excluding the 3 dB optical coupler insertion loss) as compared with Fresnel reflection, enabling the light to propagate $2 + 2$ times, in two distinct time windows, through the SMS sensor structure where it is induced intensity modulation discernible by the OTDR. By proper interfacing, this modulation becomes associated to the variation of the targeted measurand. The signal propagates in two-ways down the fiber, duplicating the sensor sensitivity.

This concept was tested adapting the SMS structure to operate as an intensity displacement sensor. One end of the SMS structure is fixed and the other one is glued to a micro positioner, which moves (displaces) horizontally introducing a curvature and losses in the SMS structure, as can be seen in Figure 2(b). The curvature presents a radius of curvature which is a function of the displacement [11]. When the displacement is applied to the SMS sensor, the ghost peak is reduced significantly when compared with the first reflection peak originated by the FLM.

In Figure 4, it is exhibited the OTDR trace for two different values of displacement related to an initial straight fiber configuration: 0.1 mm (line) and 0.7 mm (bold line). Note that the ghost signal exists (at the distance of ~23 km) in both traces and is much more sensible than the original reflection peak (at 11.6 km). In this case and for the displacements considered, the variation at the ghost peak amplitude is around 3.5 dB, while for the first reflection peak created by the FLM and for the local backscatter before and after the sensor no variation exists, essentially due to OTDR saturation effects.

The behavior of this SMS sensor structure was characterized for displacement measurement. The optical losses in the SMS sensor for the original (black dots) and ghost (red dots) peaks as a function of the displacement are presented in Figure 5. The results evidence that the ghost peak is much more sensible than the original peak for smaller values of displacement, while the original peak only starts to vary after 1.5 mm of displacement. This behavior is due to the saturation in the original peak. However, the operation dynamic range for the ghost curve is ~1 mm and for the original curve is ~2 mm. This occurs due the high global loss experienced by the ghost signal for displacements above 1 mm, turning the optical power levels close to the OTDR noise floor, while for the original signal, larger measurand induced losses are accessible considering the initial (no

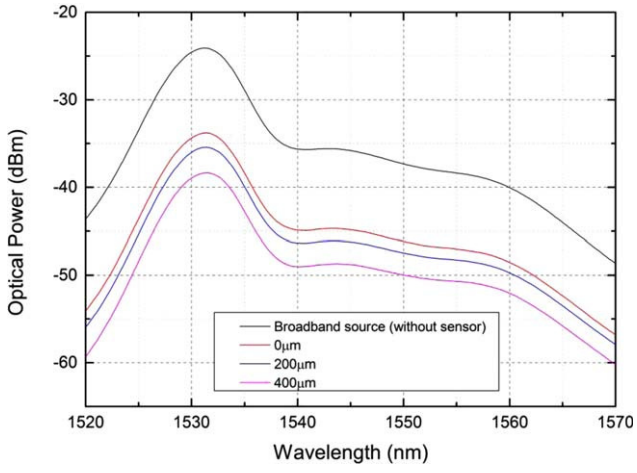

Figure 3 Optical spectra of the SMS strucuture when a broadband source illuminates it for three different values of displacement. [Color figure can be viewed in the online issue, which is available at wileyonlinelibrary.com]

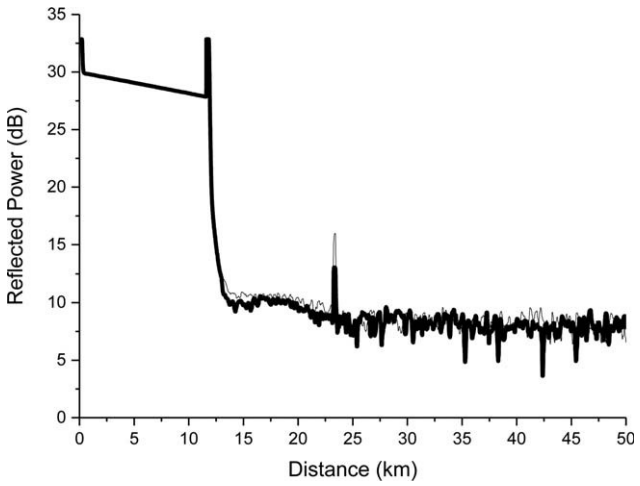

Figure 4 OTDR traces for 0.1 mm (line) and 0.7 mm (bold line) of displacement applied to the SMS sensor

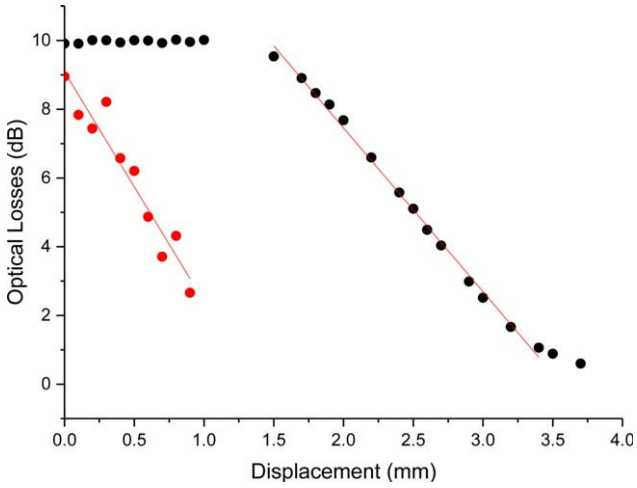

Figure 5 Optical losses for the original (black) and ghost (red) peaks as a function of the displacement applied to the SMS sensor. [Color figure can be viewed in the online issue, which is available at wileyonlinelibrary.com]

displacement) power level is also substantially larger. For displacements above 3.2 mm, the original peak seems to behave nonlinearly. Such behavior may be due to the high losses that are imposed to the sensor at these displacements levels.

Both peaks show a linear behavior with a slope of approximately −6 dB/mm for the ghost peak and approximately −4.5 dB/mm for the original peak. The resolution of the sensing head for the case of the ghost signal was evaluated by performing a step of 0.6 mm in the displacement sensor which corresponds to a 2.57 dB signal intensity variation. Considering this value and the average rms noise amplitude before and after the step change, it turns out a displacement resolution of 0.28 mm.

The results shown in Figure 5 also reveal an interesting characteristic derived from combining the processing of the sensor original and ghost signals, which is the possibility to have a larger measurement range. For smaller displacements (<1 mm), the best approach is to consider the ghost signal, while for larger values the original trace shall be considered.

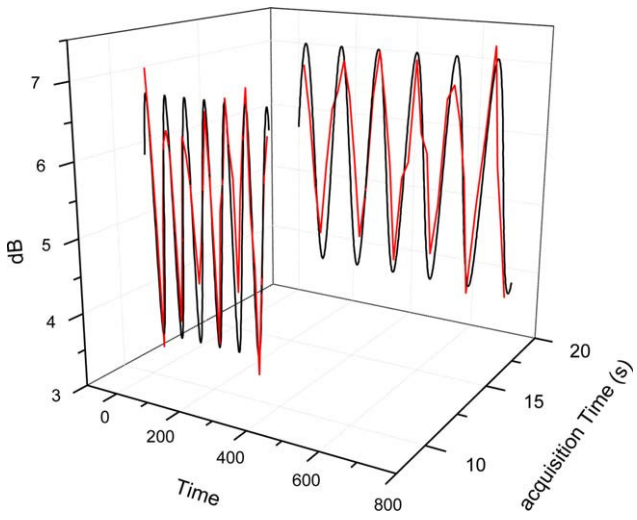

Figure 6 Response of the SMS intensity sensor associated to 6 displacement cycles with peak-to-peak amplitude of 0.6 mm occurring in time spans of 350 s and 700 s (acquisition times of 10 and 20 s, respectively). [Color figure can be viewed in the online issue, which is available at wileyonlinelibrary.com]

A further test involved to subject the sensor to a low-frequency dynamic displacement regime and to observe the detected signal. Six cycles with a peak-to-peak displacement variation of 0.6 mm (displacement from 0.1 to 0.7 mm and the way back) were applied to the sensor during two time periods, one with an extension of 350 s and the other with a time span of 700 s (corresponding to excitation frequencies of 16.7 and 7.6 mHz, respectively). For the first case the system acquisition time was set to 10 s while for the second one this value was adjusted to 20 s. The results obtained are shown in Figure 6.

It can be observed the displacement cycles originate a periodic sensor loss with a peak-to-peak amplitude of 3.5 dB, in both cases. Therefore, by adjusting the OTDR operating conditions it is possible to read time variations of the measurand (displacement in the case) within certain limits, indicating this readily applicable technique is also compatible with some level of dynamic measurement.

3. CONCLUSION

In this work, it was proposed an intensity sensor based on the ghost signal in OTDR and supported by a fiber SMS structure. To increase the ghost signal a FLM was used. The results obtained showed a linear behavior for both the original and double-reflecting signal with slopes of approximately −4.5 dB/mm and −6 dB/mm, respectively, as well as a displacement resolution of 0.28 mm. It was also found that the system is able to read periodic displacement variations in the millisecond time scale applied to the sensing head. This technique can be readily applicable in a large spectrum of situations involving remote displacement measurement, such as impact and damage detection and structural health monitoring.

ACKNOWLEDGMENT

This work was supported by project "NORTE-07-0124-FEDER-000058" which is financed by the North Portugal, Regional Operational Programme (ON.2 – O Novo Norte), under the National Strategic Reference Framework (NSRF), through the European Regional Development Fund (ERDF) and was partially supported by CAPES (Project BEX 4463/13-7) and CNPq.

REFERENCES

1. G.P. Agrawal, Fiber-optic communication systems, Wiley, West Sussex, 2002.
2. B. Glisic and D. Inaudi, Fibre optic methods for structural health monitoring, Wiley, West Sussex, 2007.
3. M.P. Gold, A.H. Hartog, and D.N. Payne, A new approach to splice-loss monitoring using long-range OTDR, Electron Lett 20 (1984), 338–340.
4. Available at: http://www.vdvworks.com/OTDR/otdrs_c.htm. Subtitle: Ghost.
5. D. Donlagic and M. Zavrsnik, Fiber-optic microbend sensor structure, Opt Lett 22 (1997), 837–839.
6. A.M. Hatta, K. Indriawati, T. Bestariyan, T. Humada, and Sekartedjo, SMS fiber structure for temperature measurement using an OTDR, Photon Sens 3 (2013), 262–266.
7. P. Di Vita and U. Rossi, Backscattering measurements in optical fibres: Separation of power decay from imperfection contribution, Electron Lett 15 (1979), 467–469.
8. D.B. Mortimore, Fiber loop reflectors, J Lightwave Technol 6 (1988), 1217–1224.
9. M.T.M.R. Giraldi, C.S. Fernandes, et al., Interrogation and multiplexing system for fiber loop mirror coupled intensity sensors using OTDR, Microwave Opt Technol Lett 56 (2014), 2860–2864.

10. D. Wang, E.A. Golovchenko, A.N. Pilipetskii, C.R. Menyuk, and Mark F. Arend, Nonlinear optical loop mirror based on standard communication fiber, J Lightwave Technol 15 (1997), 642–646.
11. J.M. Baptista, S.F. Santos, G. Rego, O. Frazão, and J.L. Santos, Micro-displacement or bending measurement using a long-period fibre grating in a self-referenced fibre optic intensity sensor, Opt Commun 260 (2006), 8–11.

INTEGRATED DECOUPLING AND MATCHING NETWORK INCORPORATED IN THE GROUND PLANE OF A COMPACT MONOPOLE ARRAY

Soumya Sheel, Mohammed M. Albannay, and Jacob C. Coetzee
School of Electrical Engineering and Computer Science, Queensland University of Technology, GPO Box 2434, Brisbane, QLD 4001, Australia; Corresponding author: s.sheel@qut.edu.au

Received 27 October 2014

ABSTRACT: *Compact arrays enable various applications such as antenna beam-forming and multi-input, multi-output (MIMO) schemes on limited-size platforms. The reduced element spacing in compact arrays introduces high levels of mutual coupling which can affect the performance of the adaptive array. This coupling causes a mismatch at the input ports, which disturbs the performance of the individual elements in the array and affects the implementation of beam steering. In this article, a reactive decoupling network for a 3-element monopole array is used to establish port isolation while simultaneously matching input impedance at each port to the system impendence. The integrated decoupling and matching network is incorporated in the ground plane of the monopole array, providing further development scope for beamforming using phase shifters and power splitters in double-layered circuits.* © 2015 Wiley Periodicals, Inc. Microwave Opt Technol Lett 57:1315–1319, 2015; View this article online at wileyonlinelibrary.com. DOI 10.1002/mop.29083

Key words: *antenna arrays; mutual coupling; decoupling network; matching network; phased arrays*

1. INTRODUCTION

Spatial diversity can significantly enhance the system capacity of wireless networks [1]. The adverse effects of mutual coupling in arrays are usually restricted using an interelement spacing of at least half a wavelength ($\lambda/2$). For antenna diversity in mobile applications, an element spacing considerably smaller than $\lambda/2$ becomes unavoidable. Reduced element spacing results in increased mutual coupling between array elements, which can decrease the antenna gain and cause significant system performance degradation [2, 3].

The effects of mutual coupling can be countered using passive, lossless decoupling, and matching networks. A decoupling network consists of interconnected reactive elements and/or transmission line sections and stubs. It provides an additional signal path between the array elements, which effectively cancels the external coupling between them. Various implementations of decoupling networks have been described in the literature [4–9]. A systematic design approach for larger circulant symmetric arrays has also been proposed [10]. The design procedure involves the repeated decoupling of the characteristic eigenmodes of the array. In most cases, additional matching networks are required to ensure an impedance match at each port.

In this article, a reactive decoupling network for a 3-element monopole array is used to establish port isolation while simultaneously matching the input impedance at each port to the system impendence. The integrated decoupling and matching network (DMN) is incorporated in the ground plane of the monopole array, providing further development scope for compact beamforming circuitry using phase shifters and power splitters on a separate substrate in a double-layered configuration.

2. INTEGRATED DMN SYNTHESIS

The 3-element uniform circular array in Figure 1 is characterized by the scattering matrix $\boldsymbol{S}^{\mathrm{a}}$, given by

$$\mathbf{S}^{\mathrm{a}}=\begin{bmatrix} S_{11}^{\mathrm{a}} & S_{12}^{\mathrm{a}} & S_{12}^{\mathrm{a}} \\ S_{12}^{\mathrm{a}} & S_{11}^{\mathrm{a}} & S_{12}^{\mathrm{a}} \\ S_{12}^{\mathrm{a}} & S_{12}^{\mathrm{a}} & S_{11}^{\mathrm{a}} \end{bmatrix}, \tag{1}$$

The corresponding admittance matrix can be calculated from

$$\mathbf{Y}^{\mathrm{a}}=Y_0(I-S^{\mathrm{a}})(I+S^{\mathrm{a}})^{-1}=\begin{bmatrix} Y_{11}^{\mathrm{a}} & Y_{12}^{\mathrm{a}} & Y_{12}^{\mathrm{a}} \\ Y_{12}^{\mathrm{a}} & Y_{11}^{\mathrm{a}} & Y_{12}^{\mathrm{a}} \\ Y_{12}^{\mathrm{a}} & Y_{12}^{\mathrm{a}} & Y_{11}^{\mathrm{a}} \end{bmatrix}, \tag{2}$$

where, $\mathbf{I}$ is a 3×3 identity matrix and Y_0 is the characteristic admittance of the system. Impedance transformation can be obtained using the circuit shown in Figure 1. It consists of three identical transmission line with a characteristic impedance Z_{01} and electrical length θ_1. Using transmission line theory the admittance matrix at Ports $1'$, $2'$, and $3'$ can be calculated from [11]

$$\mathbf{Y}'=\mathbf{B}\mathbf{A}^{-1}=\begin{bmatrix} Y'_{11} & Y'_{12} \\ Y'_{12} & Y'_{11} \end{bmatrix}, \tag{3}$$

with

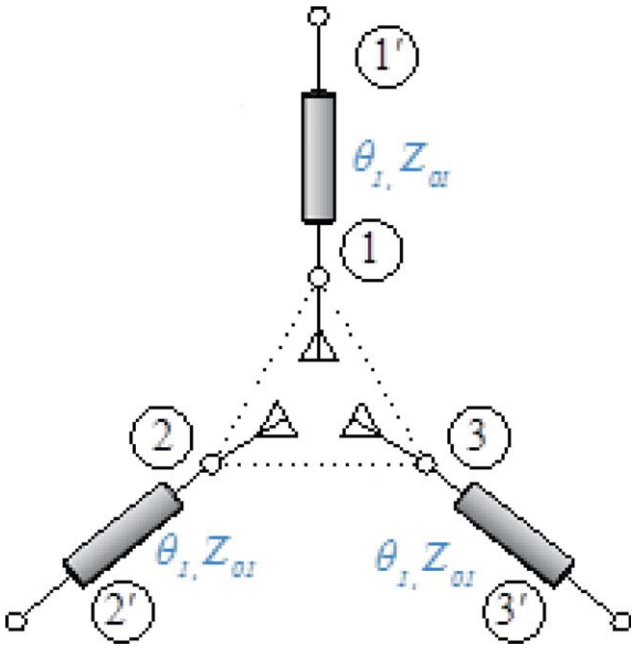

Figure 1 Impedance transforming circuit for 3-element circular array. [Color figure can be viewed in the online issue, which is available at wileyonlinelibrary.com]